

Precipitation stable isotope variability and subcloud evaporation processes in a semi-arid region

Jagoda Crawford,* Suzanne E. Hollins, Karina T. Meredith and Catherine E. Hughes

Australian Nuclear Science and Technology Organisation, Locked Bag 2001 Kirrawee DC, Sydney, NSW, 2232, Australia

Abstract:

The stable isotopic ($^2\text{H}/^1\text{H}$ and $^{18}\text{O}/^{16}\text{O}$) composition of precipitation has been used for a variety of hydrological and paleoclimate studies, a starting point for which is the behaviour of stable isotopes in modern precipitation. To this end, daily precipitation samples were collected over a 7-year period (2008–2014) at a semi-arid site located at the Macquarie Marshes, New South Wales (Australia). The samples were analysed for stable isotope composition, and factors affecting the isotopic variability were investigated. The best correlation between $\delta^{18}\text{O}$ of precipitation was with local surface relative humidity.

The reduced major axis precipitation weighted local meteoric water line was $\delta^2\text{H} = 7.20 \delta^{18}\text{O} + 9.1$. The lower slope and intercept (when compared with the Global Meteoric Water Line) are typical for a warm dry climate, where subcloud evaporation of raindrops is experienced. A previously published model to estimate the degree of subcloud evaporation and the subsequent isotopic modification of raindrops was enhanced to include the vertical temperature and humidity profile. The modelled results for raindrops of 1.0 mm radius showed that on average, the measured D-excess ($=\delta^2\text{H} - 8 \delta^{18}\text{O}$) was 19.8‰ lower than that at the base of the cloud, and 18% of the moisture was evaporated before ground level (smaller effects were modelled for larger raindrops). After estimating the isotopic signature at the base of the cloud, a number of data points still plotted below the global meteoric water line, suggesting that some of the moisture was sourced from previously evaporated water.

Back trajectory analysis estimated that 38% of the moisture was sourced over land. Precipitation samples for which a larger proportion of the moisture was sourced over land were ^{18}O and ^2H -enriched in comparison to samples for which the majority of the moisture was sourced over the ocean.

The most common weather systems resulting in precipitation were inland trough systems; however, only East Coast Lows contributed to a significant difference in the isotopic values. Copyright © 2016 Australian Nuclear Science and Technology Organisation. Hydrological Processes. © 2016 John Wiley & Sons, Ltd.

KEY WORDS deuterium; oxygen-18; precipitation; LMWL; semi-arid; Macquarie Marshes; subcloud evaporation; Murray–Darling Basin

Received 8 December 2015; Accepted 12 April 2016

INTRODUCTION

The stable isotopic ($^2\text{H}/^1\text{H}$ and $^{18}\text{O}/^{16}\text{O}$) composition of precipitation has been used for a variety of hydrological studies, e.g. groundwater and surface water mixing, and the study of atmospheric processes (e.g. Awad, 1996; Clark and Fritz, 1997; Gat, 2000; Gat and Airey, 2006; Yoshimura *et al.*, 2010). For monthly to inter-annual timescales, relationships between the stable isotopes of precipitation and climatic variables can be studied using the Global Network of Isotopes in Precipitation data (e.g. Dansgaard, 1964; IAEA, 1992; Araguás-Araguás *et al.*, 2000). Higher frequency data, such as presented here, can be used to study such aspects as the relationship between precipitation isotopes and moisture sources and synoptic

weather systems, which is difficult to achieve using monthly averaged values (e.g. Friedman *et al.*, 2002; Burnett *et al.*, 2004; Sjoström and Welker, 2009; Crawford *et al.*, 2013). Present-day relationship between climatic variables and stable isotopes can be used to infer past climatic conditions, for example, using such paleorecords as stalagmites and ice cores (Dansgaard *et al.*, 1993; Bar-Matthews *et al.*, 1997; Tan, 2014).

Studies of high frequency variability of $\delta^{18}\text{O}$ in precipitation in the Australian region include sites in Tasmania (Treble *et al.*, 2005; Barras and Simmonds, 2008), Melbourne (Barras and Simmonds, 2009), Adelaide (Guan *et al.*, 2009, 2013) and four sites in the Sydney region (Hughes and Crawford, 2013). However, until now, a long-term high frequency data set was not available for an inland Australian semi-arid region. This study analyses a 7-year record of the isotopic composition of daily precipitation samples at the Macquarie Marshes. The Macquarie Marshes are located in semi-arid North

*Correspondence to: Jagoda Crawford, Australian Nuclear Science and Technology Organisation, Locked Bag 2001 Kirrawee DC, Sydney, NSW 2232, Australia.
E-mail: Jagoda.Crawford@ansto.gov.au

west New South Wales (NSW), Australia. The Macquarie Marshes Nature Reserve, with an area of ~200 km², was created in 1971. It is one of the largest remaining inland semi-permanent wetlands in south-eastern Australia and is of international importance, being listed as a Ramsar site since 1986 (Wen *et al.*, 2013, and references therein). The average precipitation to potential evapotranspiration ratio, or aridity index, in this region is approximately 0.35, resulting in high evaporative losses from surface water bodies and corresponding isotopic enrichment of residual water.

Given the $\delta^2\text{H}$ and $\delta^{18}\text{O}$ composition of a precipitation sample, the deuterium excess of the sample can be calculated as $\text{D-excess} = \delta^2\text{H} - 8 \delta^{18}\text{O}$ (Dansgaard, 1964). The D-excess is influenced by the conditions at the moisture source; generally, there is a negative correlation between D-excess and relative humidity and a positive correlation with sea surface temperature (Dansgaard, 1964; Merlivat and Jouzel, 1979; Uemura *et al.*, 2008). Using this relationship, D-excess has been used in many studies to determine the temporal changes in moisture supply for a given location (e.g. Vimeux *et al.*, 2001). D-excess is also commonly used as an indicator of the extent of evaporation of raindrops below the cloud base under warm dry conditions (which reduces the D-excess of the rainfall) and moisture recycling by evaporation from overland water bodies (which may increase the D-excess of the rainfall), (Jacob and Sonntag, 1991; Froehlich *et al.*, 2008; Peng *et al.*, 2010). Recently, Froehlich *et al.* (2008) and later Kong *et al.* (2013) used the model developed by Stewart (1975) to quantify the effect of subcloud evaporation on the D-excess of event-based precipitation.

At the Macquarie Marshes, it is expected that subcloud evaporation will be a major driver in this terrestrial system; therefore, the influence of subcloud evaporation of raindrops on D-excess variation in rainfall isotope data is assessed using the methodology described in Kong *et al.* (2013) with one enhancement. As the distance from the base of the cloud to the ground can be large and temperature and humidity can vary over this distance, the model was modified to take into account the vertical variation of temperature and humidity. It is anticipated that our high-frequency data set will provide a means for estimating the subcloud effect on the D-excess of precipitation for the first time for a site in the Murray–Darling Basin. The study is particularly significant as it provides much needed isotopic rainfall input data to provide greater certainty for hydrological models in this important food production area of Australia.

We use the 7-year data set of daily precipitation to develop a local meteoric water line (LMWL) for the Macquarie Marshes. We also assess the variability in rainfall stable isotopes with regard to (1) seasonality, (2) climatic variables, (3) synoptic weather systems and (4) land and oceanic moisture sources. In addition, we

modify the model of Kong *et al.* (2013) and use the modified model to quantify the impact of below cloud evaporation on D-excess of precipitation. This then allows us to identify whether other processes such as overland moisture sources are leading to low D-excess values in rainfall at this semi-arid site.

The outcomes from this study can be used as input data for hydrological modelling and an understanding of the dominant processes in semi-arid climatic regions across the world. This information can also be used in paleoclimate records interpretation.

METHODS AND DATA

Study site

The Macquarie Marshes are located in the north west of NSW on the western side of the Great Dividing Range (Figure 1). The region has a semi-arid climate with low precipitation (annual precipitation of 447.1 mm), hot summers (mean maximum temperature of 34.6 °C) and cold winters (mean minimum temperature of 4.0 °C; BOM, 2015; Wen *et al.*, 2013). The sampling site is located at the southern edge of the marshes at 30.89°S, 147.49°E and 153 mAHD (Australian Height Datum).

The long-term (1900 to 2014) average monthly precipitation and mean monthly minimum and maximum temperatures at the nearby Bureau of Meteorology (BOM) site, Quambone Station (site no. 051042 located at 30.93°S, 147.87°E and 152 m above sea level), are presented in Figure 2. Marginally higher precipitation amounts occur in the summer months, with the highest long-term monthly mean precipitation occurring in January (50.6 mm) and the lowest in August (27.1 mm). The average number of annual rain days is 45 spread fairly uniformly across the year.

Potential areal evapotranspiration (~1300 mm per annum; BOM http://www.bom.gov.au/jsp/ncc/climate_averages/evapotranspiration/) exceeds the annual precipitation by a factor of three in this region. However, the extent of evaporation varies over the year, with maximum potential evaporation occurring in summer together with the higher precipitation months.

It is unlikely that diffuse rainfall recharge contributes significantly to groundwater in this semi-arid environment because the high evaporation rates and presence of impermeable clay-rich soils would make it difficult for small volumes of rainfall to recharge the shallow aquifer and form groundwater (Meredith *et al.*, 2015). It is therefore presumed that the majority of local precipitation is subject to evapotranspiration following rainfall events. Surface water in the Macquarie Marshes is generally sourced from upstream, rather than local runoff, including allocated environmental releases from Burrendong Dam more than 200 km to the south east.

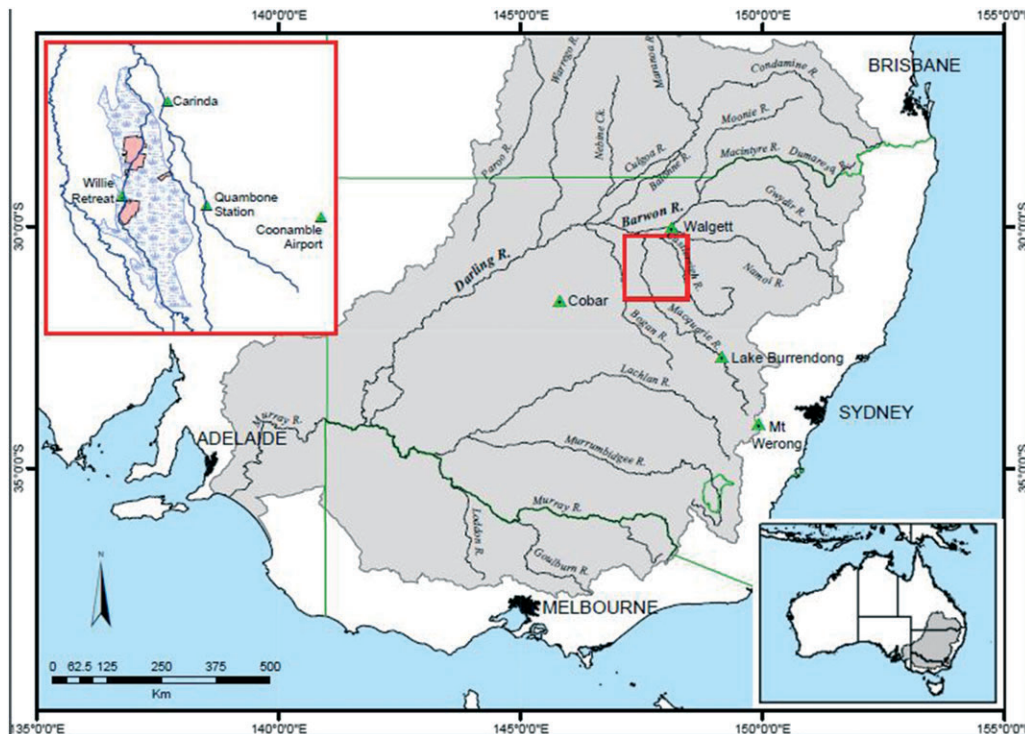


Figure 1. Location of the Macquarie Marshes and key data source and comparison sites referred to in the text. In the inset, the Macquarie Marshes Nature Reserve is shaded red, and the extent of the floodplain wetland during infrequent periods of inundation is indicated in blue hatching. The Murray Darling Basin is shaded grey

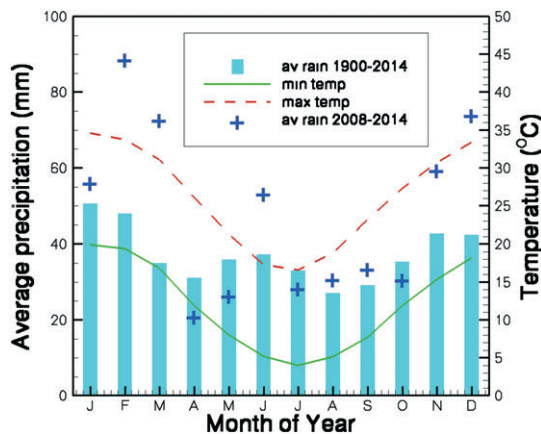


Figure 2. The monthly mean precipitation and mean minimum and maximum temperatures at Quambone, (means calculated from 1900 to 2014). Also presented, by crosses, is the monthly average precipitation for the sampling period (February 2008 to December 2014)

Precipitation sample collection

Daily precipitation samples were collected from February 2008 to December 2014 (a total of 284 samples, two of which were rejected based on precipitation amount of 1 mm and high values of $\delta^{18}\text{O}$ and $\delta^2\text{H}$, indicating possible evaporation in the sampler) at Macquarie Marshes (Willie Retreat; BOM station no. 51084), lat 30.89°S , long 147.49°E , elevation 153 m AHD. Rainfall samples were collected daily after rain

events from a rainfall sampler designed to minimize evaporation as described by Hughes and Crawford (2013) and stored unpreserved in high-density polyethylene bottles. The monthly average precipitation for this period is shown by the crosses in Figure 2. Generally, higher precipitation averages were seen for the sampling period as compared with the long term averages, particularly for the warmer months. This is largely because of the sampling period being dominated by La Niña periods (2007–2008, 2010–2011 and 2011–2012). On the other hand, only one moderate El Niño period (2009–2010) was recorded over the sampling interval (NWS, 2015).

Other meteorological variables were not available at the site; hence, measurements from the nearest BOM sites were used. Air temperature was sourced from Quambone Station (BOM station no. 051042, located at 36 km from sampling site). The relative humidity was calculated using temperature and dew point temperature, which were sourced from Coonamble Airport – BOM station no. 051161 (located at 85 km from the sampling site).

Isotope analyses for the samples collected prior to November 2008 were undertaken at the CSIRO Adelaide laboratories using IRMS, with a reported accuracy of ± 1.0 and $\pm 0.15\text{‰}$ for $\delta^2\text{H}$ and $\delta^{18}\text{O}$ respectively (March samples only) or cavity ring-down spectroscopy on a Los Gatos LGR DLT-100 with a reported accuracy of ± 0.6

and $\pm 0.2\%$ for $\delta^2\text{H}$ and $\delta^{18}\text{O}$ respectively. From November 2008 to May 2010, analyses were conducted at the Alberta Research Council laboratories using isotope ratio mass spectrometry with a reported accuracy of ± 1.0 and $\pm 0.2\%$ for $\delta^2\text{H}$ and $\delta^{18}\text{O}$ respectively. All the samples collected from June 2010 onwards were analysed using a cavity ring-down spectroscopy method on a Picarro L2120-I Water Analyser (reported accuracy of ± 1.0 , $\pm 0.2\%$ for $\delta^2\text{H}$ and $\delta^{18}\text{O}$ respectively). All of these laboratories run a minimum of two in-house standards calibrated against VSMOW/VSMOW2 and SLAP/SLAP2 with samples in each batch. All isotope results are reported as per mil (‰) deviations from the international standard, Vienna Standard Mean Ocean Water. Detailed descriptions of the methods are included with the sample data in the Supplementary material.

Back trajectory and trajectory meteorological data

Locations of moisture sources and large scale rainout from an air mass, before reaching a sampling site, can be identified using back trajectories and meteorological information along the back trajectories (e.g. Friedman *et al.*, 2002; IAEA, 2005; Barras and Simmonds, 2008; Sodemann *et al.*, 2008; Sjoström and Welker, 2009; Vachon *et al.*, 2010). Back trajectories in the current study were generated using Hybrid Single-Particle Lagrangian Integrated Trajectory (HYSPLIT; Draxler and Rolph, 2003), with the $1^\circ \times 1^\circ$ meteorological data set which is generated by the global data assimilation system (GDAS) model run by the US National Weather Service's National Centre for Environmental Prediction. To examine moisture sources and rainout, we use the location of the back trajectories, the altitude of trajectories, relative humidity, planetary boundary layer height and precipitation, as calculated by the HYSPLIT model at each point along the back trajectory. These variables are interpolated by HYSPLIT from the GDAS data sets, which are available at <ftp://arlftp.arlhq.noaa.gov/archives/gdas1>.

To determine the source of moisture, the method of Sodemann *et al.* (2008) was implemented. This involves generating a vertical profile of the relative humidity at the site from the GDAS data then calculating the back trajectory starting at the lowest altitude where the relative humidity was $>80\%$ (as used by Sodemann *et al.*, 2008). On the examination of the vertical profiles of relative humidity, the lowest altitude at which the relative humidity was greater than 80% was between 1500 m above mean sea level (m.s.l.) and 2000 m (m.s.l.), and as a result, an altitude of 1750 m (m.s.l.) was chosen for back trajectory calculations. Further, as the hour of day on which the precipitation occurred was not available, a back trajectory for each hour of the day was generated, and average values were used.

The locations of surface moisture sources were identified as points along the back trajectory where absolute humidity increased by more than $0.04 \text{ g kg}^{-1} \text{ h}^{-1}$ and when the air mass was within the planetary boundary layer, according to Sodemann *et al.* (2008). When the absolute humidity was below 0.05 g kg^{-1} , it was assumed that no previously sourced moisture contributed to the current precipitation event (Sodemann *et al.*, 2008; Baldini *et al.*, 2010). Ten-day back trajectories were used (corresponding to a mean residence time of water in the atmosphere of about 10 days; Trenberth, 1998; Gat, 2000; Friedman *et al.*, 2002), and at locations where moisture was evaporated from the surface, the relative humidity and temperature at surface level were extracted from HYSPLIT. The cumulative precipitation from the air mass prior to the sampling site was also calculated as the sum of precipitation along the back trajectory prior to reaching the site and starting from the last point where moisture was sourced for the current event.

For each back trajectory, moisture could be sourced from more than one location along the back trajectory, and this moisture was integrated along the back trajectory (say *tot_moisture*). Integration was also performed only for moisture sourced while the back trajectory was over land, and then using *tot_moisture*, the fraction of the moisture sourced from over land was determined. The reported fraction of moisture sourced over land was the precipitation amount weighted average from all sampling days.

Synoptic weather classification

A synoptic weather classification scheme was used to investigate the isotopic composition of precipitation by synoptic weather system type. For this study, a slightly modified synoptic weather classification scheme to that in Crawford *et al.* (2013) was used to investigate the isotopic composition of precipitation. Five of the weather systems from Crawford *et al.* (2013) were selected:

- East Coast Low – closed cyclonic low-pressure systems off the east coast of Australia (ECL: Speer *et al.*, 2009, referred to as offshore lows in Matthews and Geerts, 1995), the centres of which vary in latitude along the east coast.
- Offshore high – where an offshore high-pressure system is located to the east or southeast of the site, occurring both in winter and summer.
- Inland trough – these occur more often in non-winter months. Their location varies over the continent.
- Pre-frontal – pre-frontal troughs and pre-frontal systems as described in Crawford *et al.* (2013) are grouped in this system type. The decision was made to group these two systems together, as precipitation from

frontal systems is less frequent at the Macquarie Marshes, and the difference in isotopic values in precipitation from these two systems was low in the previous study.

- Post-frontal – where precipitation occurred during and immediately after the passage of the front.

In addition, local low pressure systems were identified separately for this site when overland low pressure systems were identified to distinguish them from inland troughs. The reader is referred to Matthews and Geerts (1995) and Crawford *et al.* (2013) for mean sea-level pressure maps for the different synoptic types considered.

To identify the weather systems resulting in precipitation at the site, mean sea-level pressure maps were used (BOM, 2012).

RESULTS AND DISCUSSION

Stable isotope distribution

Histograms representing the number of samples in each specified range of the $\delta^{18}\text{O}$ and $\delta^2\text{H}$ values of the daily precipitation samples are presented in Figure 3. The range of the $\delta^{18}\text{O}$ values was from -15.08 to 5.39‰ with an arithmetic mean of -3.14‰ (precipitation weighted mean of -4.04‰), while the $\delta^2\text{H}$ range was from -107.9 to 39.0‰ with an arithmetic mean of -15.5‰ (precipitation weighted mean of -20.1‰). The precipitation weighted mean values are similar to a NSW coastal site, Lucas Heights (located 480 km to the south-east; Hughes and Crawford, 2013). However, these similar values result from different processes; e.g. at Lucas Heights, being located close to the coast, there would be little depletion of isotopes as a result of the continental effect, whereas at the Macquarie Marshes, one contributing process would be subcloud evaporation of raindrops (which results in ^{18}O and ^2H -enriched rainfall), which is more likely a result of the higher summer temperatures and lower

rainfall amounts. The resulting low D-excess is the reason for the observed skew in the $\delta^2\text{H}$ distribution.

The distributions of the $\delta^{18}\text{O}$ values and D-excess by month of year are presented in Figure 4. Higher $\delta^{18}\text{O}$ values were seen during the summer months, consistent with Feng *et al.* (2009), where maximum $\delta^{18}\text{O}$ values were found in the summer months for sites located poleward of 30° in the Global Network of Isotopes in Precipitation. In our data, a considerable variation of $\delta^{18}\text{O}$ was seen within each month and particularly in the warmer months.

The D-excess values ranged from -16.3 to 23.4‰ with a mean of 9.6‰ and a precipitation weighted mean of 12.3‰ . The precipitation weighted average D-excess is lower than those reported for the Sydney Basin (Hughes and Crawford, 2013; where the range of D-excess was from 15.64 to 18.33‰ for sites located to the east of the Great Dividing Range at a distance from 380 to 480 km from our site.). Hence, the difference between moisture sourced over land and moisture sourced over the oceans was investigated (Local and Oceanic Moisture Sources section).

Stable isotope variability

The relationships between the isotopic composition of precipitation and climatic variables have been used in a number of studies to infer the past atmospheric conditions using rainfall records, such as from speleothems and ice cores (Dansgaard *et al.*, 1993; Bar-Matthews *et al.*, 1997). For example, the isotopic composition of the record has been used to infer past precipitation amounts in tropical areas and past temperature at higher latitudes (Noone and Simmonds, 2002). However, statistically significant relationships of $\delta^{18}\text{O}$ and air temperature or precipitation amounts are not readily identified from the measured values alone. Hence, in this study, we investigate the relationships between rainfall stable isotopes and climatic variables to allow climatic interpretations to be made more readily, for example, in groundwater studies.

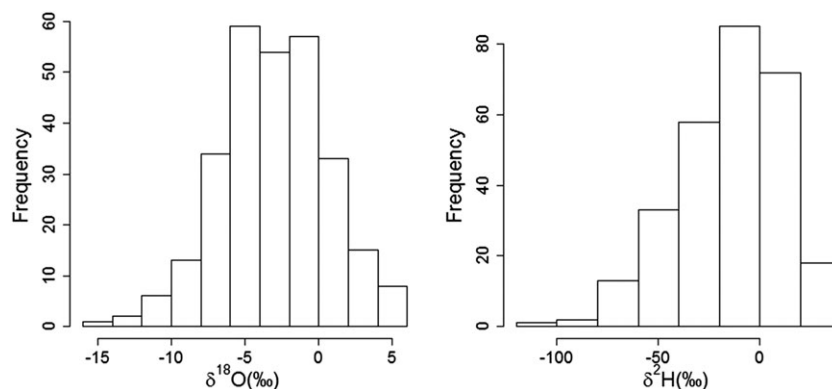


Figure 3. Histograms, representing the number of samples in each range, of $\delta^{18}\text{O}$ and $\delta^2\text{H}$ in the daily precipitation samples of the Macquarie Marshes

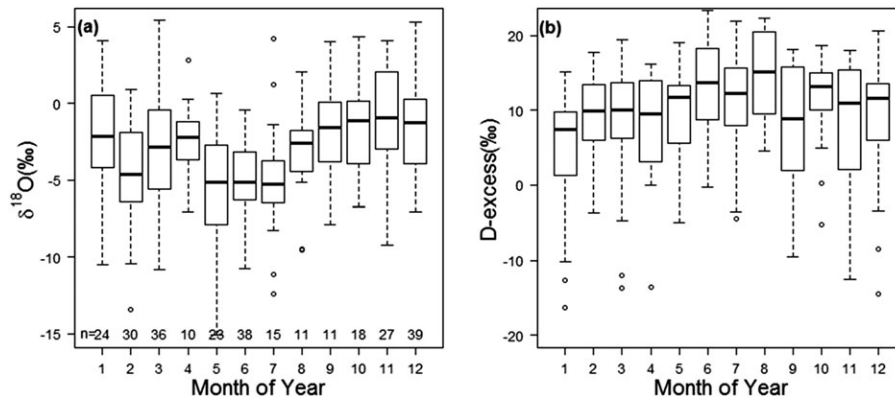


Figure 4. Distribution of $\delta^{18}\text{O}$ and D-excess with time of year at the Macquarie Marshes. The number of samples in each month is presented at the base of (a). Boxes represent the 25th and 75th percentiles, the median is represented by the line through the box, whiskers represent the 10th and 90th percentiles, and extreme events are indicated by open circles

Precipitation amount. A regression fit of $\delta^{18}\text{O} = -0.06 \times P - 2.4\text{‰}$ was obtained (where P is the precipitation amount), with a very low r^2 value (0.05), indicating that precipitation amount is not a controlling factor of the isotopic composition of precipitation at this site, particularly when smaller precipitation amounts are taken into account. However, plotting $\delta^{18}\text{O}$ against the precipitation amount, Figure 5 shows that 92% of the measurements lie below a line with slope of -0.17 and an intercept of 4, which was fitted by visual inspection to illustrate that larger volume precipitation is unlikely to be more ^{18}O and ^2H -enriched relative to low volume precipitation.

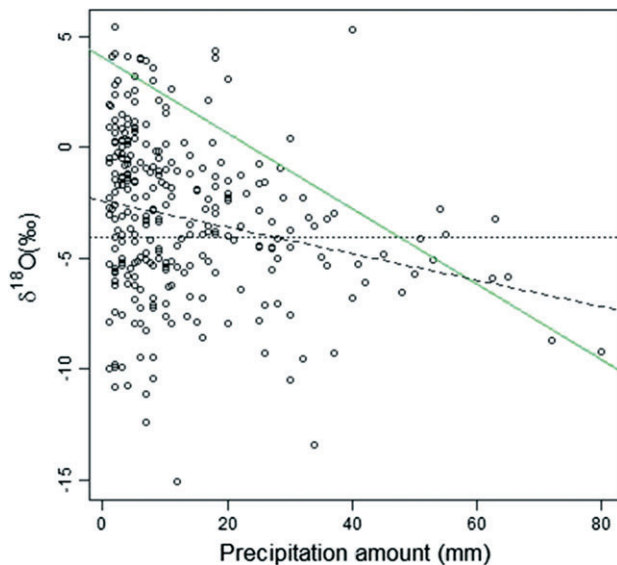


Figure 5. $\delta^{18}\text{O}$ vs precipitation amount (with regression line dotted in black $\delta^{18}\text{O} = -0.06P - 2.4$) for the Macquarie Marshes. The bounding line (line in green $\delta^{18}\text{O} = -0.17P + 4$) was fitted by inspection which best represented the fact that the $\delta^{18}\text{O}$ of precipitation was unlikely to be high for larger precipitation amounts

Meteorological parameters. Correlation analysis of the local surface temperature, local surface relative humidity and a number of HYSPLIT-generated parameters (either conditions at the moisture source or along the back trajectory) with $\delta^{18}\text{O}$ and D-excess was undertaken (Table I). The best correlation both for $\delta^{18}\text{O}$ and D-excess was obtained with local surface relative humidity (Table I and Figure 6). A negative correlation between local surface relative humidity and $\delta^{18}\text{O}$ and a corresponding positive correlation with D-excess (both with a p -value of less than 0.01) indicate that the subcloud evaporation of raindrops has a significant effect on the isotopic composition of precipitation at the study site, as subcloud evaporation results in enriched precipitation with a lower D-excess, and more evaporation occurs under drier conditions. This is also supported by the correlation with local surface temperature, albeit weak (although with a p -value of less than 0.01; (e.g. Peng *et al.*, 2007), as higher temperatures promote re-evaporation of raindrops. Regression equations between $\delta^{18}\text{O}$ (and D-excess) and the selected variables are presented in Table II. About 30% of the variation in $\delta^{18}\text{O}$ can be explained by the local surface relative humidity, which can be increased to 34% if we also include relative humidity at the moisture source in the regression equation.

The next highest correlations were between $\delta^{18}\text{O}$ and the air mass cumulative rainout prior to the site (which reflects the rainout effect) and also the relative humidity at the moisture source and along the back trajectory. The rainout effect is a result of the well-known Rayleigh process (Dansgaard, 1964), and thus, a correlation between air mass cumulative rainout prior to the site and $\delta^{18}\text{O}$ has been seen at other sites, e.g. at Mt Werong (Crawford *et al.*, 2013; Samuels-Crow *et al.*, 2014).

When monthly precipitation-weighted quantities were considered, the correlation was lower for conditions along the back trajectory and the temperature at the

Table I. Correlation coefficient (r) between $\delta^{18}\text{O}$ (and D-excess) and selected parameters for precipitation in the Macquarie Marshes

Parameter	Individual samples		Monthly precipitation weighted	
	Correlation with $\delta^{18}\text{O}$	Correlation with D-excess	Correlation with $\delta^{18}\text{O}$	Correlation with D-excess
Local surface relative humidity	-0.55	0.39	-0.62	0.43
Relative humidity at the moisture source ^a	-0.40	0.14	-0.28	0.11*
Air mass prior cumulative rainfall ^a	-0.42	0.18	-0.31	0.17*
Relative humidity along the back trajectory ^a	-0.38	0.18	-0.21	0.09*
Local surface temperature	0.37	-0.28	0.36	-0.34
Temperature at the moisture source ^a	0.31	-0.22	0.23	-0.29

^a Derived using HYSPLIT from the gridded GDAS meteorological files; the other parameters were derived from the Coonamble Airport BOM site.

*Significant at 99% confidence level (p -value = 0.01).

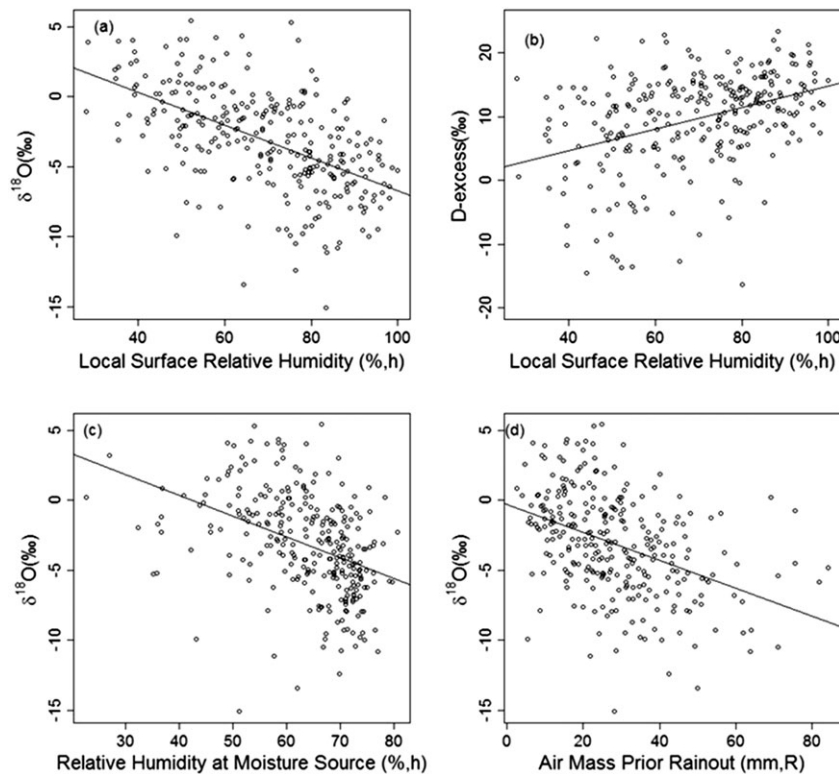


Figure 6. Regression of a) local surface relative humidity with $\delta^{18}\text{O}$ ($\delta^{18}\text{O} = -0.11h + 4.9$, $r^2 = 0.30$; and b) D-excess ($\text{D-excess} = 0.16h - 2.1$, $r^2 = 0.15$; c), $\delta^{18}\text{O}$ with relative humidity at the moisture source ($\delta^{18}\text{O} = -0.15h + 6.23$, $r^2 = 0.16$; and d) $\delta^{18}\text{O}$ and prior rainout ($\delta^{18}\text{O} = -0.1R - 0.32$, $r^2 = 0.17$; d) for precipitation from the Macquarie Marshes. The p -value in all cases was less than 0.01

moisture source. One factor that could contribute to this is the potential large variation of conditions in the air mass for the samples collected in the same month, which would be reduced when the average values are considered. The only improvement was seen for local surface relative humidity, which is generally seasonally controlled and not subject to spatial variation seen in trajectory related parameters.

Isotopic variability as a result of synoptic weather systems

In many parts of the world, it has been found that the isotopic composition of precipitation can be influenced by the prevailing synoptic weather systems (e.g. Dansgaard, 1964; Gedzelman and Lawrence, 1990; Clark and Fritz, 1997; Gedzelman *et al.*, 2003; Scholl *et al.*, 2009; Baldini *et al.*, 2010; Windhorst *et al.*, 2012; Guan *et al.*, 2013;

Table II. Regression between $\delta^{18}\text{O}$ (and D-excess) and selected parameters for precipitation at the Macquarie Marshes

Parameter	Individual samples		Monthly precipitation weighted	
	$\delta^{18}\text{O}=\text{}$	D-excess=	$\delta^{18}\text{O}=\text{}$	D-excess=
Local surface relative humidity (LH)	-0.11LH + 4.9 (0.30)	0.17LH - 2.1 (0.15)	-0.1LH + 5.6 (0.38)	0.18LS - 1.3 (0.19)
Relative humidity at the moisture source (SH ^a)	-0.15SH + 6.2 (0.16)	0.10SH - 3.0 (0.08)	-0.13SH + 4.7 (0.08)	0.10SH + 4.3 (0.02)
Air mass prior cumulative rainfall (PR ^a)	-0.1PR - 0.32 (0.17)	0.09PR + 7.1 (0.03)	-0.09PR - 0.6 (0.10)	0.09PR + 7.9 (0.03)
Humidity along the back trajectory (TH ^a)	-0.13TH + 4.8 (0.14)	0.13TH + 2.05 (0.03)	-0.10TH + 2.8 (0.05)	0.08TH + 5.8 (0.01)
Local surface temperature (LT)	0.24LT - 8.1 (0.14)	-0.38LT + 17 (0.07)	0.23LT - 7.7 (0.13)	-0.4LT + 18.7 (0.12)
Temperature at the moisture source (ST ^a)	0.21ST - 7.7 (0.10)	-0.31LT + 16.3 (0.04)	0.16ST - 6.5 (0.06)	-0.38ST + 18.6 (0.09)
LH + SH	-0.09LH - 0.08SH + 8.9 (0.34)	0.17LH - 0.01SH - 1.8 (0.15)	-0.02LH - 0.13SH + 6.9 (0.39)	0.19LH - 0.04SH + 0.9 (0.20)

The r^2 values are presented in brackets.

^a Parameter was derived using HYSPLIT from the gridded GDAS meteorological files; the other parameters were derived from the Coonamble Airport BOM site.

and Sinclair *et al.*, 2013). For the Sydney region, Crawford *et al.* (2013) found that the arithmetic mean $\delta^{18}\text{O}$ associated with ECLs was significantly lower than that associated with other synoptic weather systems (with a p -value of 0.05). Here, we investigate the isotopic difference between precipitation events resulting from different weather systems for this inland semi-arid site.

Each day, for which precipitation was sampled, was classified according to the synoptic weather systems presented in the Synoptic Weather Classification section. The number of occurrences of each synoptic weather system by season is presented in Table III, and the distributions of $\delta^{18}\text{O}$, $\delta^2\text{H}$, D-excess and sample precipitation amount by synoptic weather system are presented in Figure 7. Over the sampling period, inland troughs

were the most common weather systems resulting in precipitation at the Macquarie Marshes, with their highest occurrence in summer. Least common weather systems to contribute to precipitation at the Macquarie Marshes were ECLs and post-frontal followed by pre-frontal trough systems. As in Crawford *et al.* (2013), the ECLs resulted in the most ^{18}O and ^2H -depleted precipitation. However, the precipitation amount from ECLs was low at this site (Figure 6d). The site is located further inland and on the western side of the Great Dividing Range; hence, little impact is seen from the ECLs which are centred over the ocean off the east coast. Also, the precipitation weighted average values for the ECLs were dominated by one sample with a precipitation amount of 22 mm, which was ^{18}O and ^2H -depleted relative to the other samples.

Table III. The number of samples classified in each synoptic weather type, by season. Also presented are the precipitation weighted average $\delta^{18}\text{O}$, $\delta^2\text{H}$ and D-excess for precipitation at the Macquarie Marshes

System	Autumn	Winter	Spring	Summer	$\delta^{18}\text{O}$	$\delta^2\text{H}$	D-excess
East Coast Low (ECL)	1	4	1	3	-6.25	-37.10	12.92
Local low (LL)	13	13	13	18	-4.25	-20.78	13.18
Offshore high (High)	17	7	1	11	-4.72	-25.99	11.86
Inland trough (Tr)	29	22	28	50	-4.04	-20.12	12.18
Pre-frontal trough (PFT)	7	8	8	7	-4.62	-23.43	13.50
Post-frontal (PF)	0	5	1	3	0.47	9.57	5.82

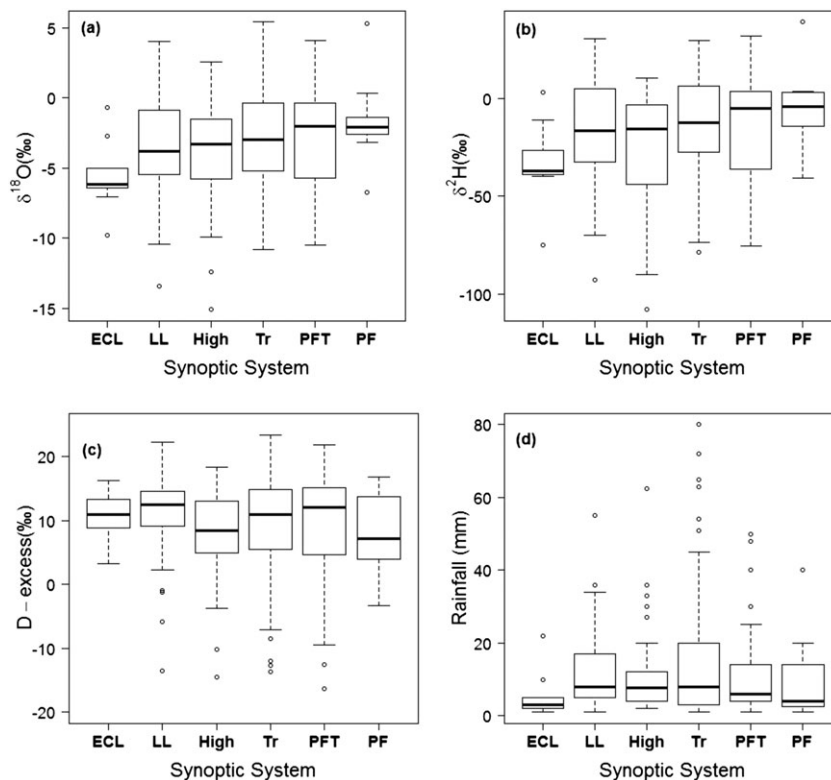


Figure 7. Box and whisker plots of $\delta^2\text{H}$, $\delta^{18}\text{O}$, D-excess and sample precipitation amount by synoptic weather system; East Coast Low (ECL), local low (LL), high (High), inland trough (Tr), pre-frontal trough (PFT) and post-frontal (PF). Boxes and whiskers as in Figure 4

A Welch test (i.e. a *t*-test for the significance in the difference of the means of two populations when their variances are unequal) was undertaken to see if the differences in the mean $\delta^{18}\text{O}$ between systems were significant. The difference was significant at 95% confidence level only between the ECLs and most other systems (aside from high-pressure systems), indicating a small difference in the isotopic signature between the other synoptic weather systems. On the other hand, there was little difference in the median D-excess between the synoptic weather systems, indicating that processes unrelated to the synoptic weather systems affect the D-excess at this site.

The precipitation weighted average isotopic values for each synoptic type are presented in Table III. The results for the post-frontal systems were affected by one sample with a high precipitation amount, and thus, post-frontal systems are not considered further. Of the remaining systems, inland troughs resulted in the most ^{18}O and ^2H -enriched precipitation weighted isotopic composition with a relatively lower D-excess.

These results show that the synoptic weather systems have a small influence on the isotopic signature of precipitation at this semi-arid site, and rainout, conditions at the moisture source, and conditions at the sampling site appear to be more important (from the correlation coefficients in Table I).

Local meteoric water line

Using precipitation weighted reduced major axis regression (Crawford *et al.*, 2014), the LMWL was calculated to be $\delta^2\text{H} = 7.20 \delta^{18}\text{O} + 9.2$. When using precipitation weighted least squares regression, the slope is higher than that using ordinary least squares regression (OLSR; Table IV). The slope of OLSR-developed LMWLs tends to be lower than when precipitation weighted reduced major axis regression is used for regions where subcloud evaporation impacts on rainfall. This is because smaller samples which are more likely to be impacted by subcloud evaporation tend to have a smaller D-excess and when fitted using OLSR have the same weighting in the fitting process. When precipitation weighted regression is used, the larger precipitation events, which are more hydrologically

important, have a larger influence on the fit (Hughes and Crawford, 2012; Crawford *et al.*, 2014). Nevertheless, the slope and intercept for both least square approaches are lower than the GMWL ($\delta^2\text{H} = 8 \delta^{18}\text{O} + 10$; Craig, 1961; note that the GMWL was developed using the OLSR technique; thus, it is more appropriate to compare the OLSR-derived LMWL with the GMWL). This trend is not unique; a lower slope and intercept was also found for the semi-arid region of the US Great Plains (Harvey and Welker, 2000) and an arid region in northwest China (Pang *et al.*, 2011) and has been discussed by Hughes and Crawford (2012) and Crawford *et al.* (2014). Lower slope and intercept have also been observed for the OLSR-LMWL at Cobar (Australia) for 2007 to 2013 ($\delta^2\text{H} = 6.97 \delta^{18}\text{O} + 8.3$; Meredith *et al.*, 2015) developed from monthly precipitation samples. The climate at Cobar is hot and persistently dry; thus, subcloud evaporation would be a contributing factor.

When we plotted $\delta^2\text{H}$ against $\delta^{18}\text{O}$, two main groupings of data were evident (Figure 8) – the data that plotted on the GMWL (most of the winter precipitation)

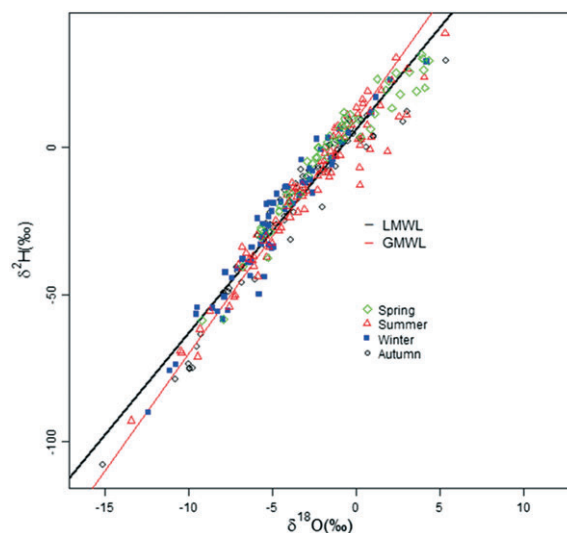


Figure 8. The calculated ordinary least square regression local meteoric water line (2008–2014, $\delta^2\text{H} = 6.96 \delta^{18}\text{O} + 6.4$, $r^2 = 0.94$, p -value = 0.00), global meteoric water line ($\delta^2\text{H} = 8 \delta^{18}\text{O} + 10$) and individual samples for precipitation for the Macquarie Marshes

Table IV. Local meteoric water lines

	LMWL (PWRMA)	LMWL (OLSR)
Summer	$\delta^2\text{H} = 7.26 (0.14) \delta^{18}\text{O} + 7.6 (0.7)^*$	$\delta^2\text{H} = 6.87 (0.2) \delta^{18}\text{O} + 5.1 (0.8)$
Winter	$\delta^2\text{H} = 8.31 (0.28) \delta^{18}\text{O} + 17.9 (1.6)$	$\delta^2\text{H} = 7.44 (0.24) \delta^{18}\text{O} + 10.2 (1.4)$
Annual	$\delta^2\text{H} = 7.20 (0.1) \delta^{18}\text{O} + 9.1 (0.5)^*$	$\delta^2\text{H} = 6.96 (0.11) \delta^{18}\text{O} + 6.4 (0.5)$
Monthly precipitation weighted	$\delta^2\text{H} = 7.24 (0.2) \delta^{18}\text{O} + 9.2 (0.9)$	$\delta^2\text{H} = 7.06 \delta^{18}\text{O} + 7.6 (0.9)$

The standard errors of the estimated parameters are reported in ‘()’.

*Indicates that the difference in slope between OLSR and PWRMA was significant at 95% confidence interval.

and the data that plotted below the GMWL (which was mostly for the warmer months; November to March). The latter can be explained because small precipitation amounts (under warm conditions) are subject to subcloud evaporation (Dansgaard, 1964) and plot below the GMWL. Of the 282 samples, 32% of the samples had precipitation of less than 5 mm, and of these, 44% were associated with a local surface temperature of 20 °C or more – favourable conditions for subcloud evaporation. In the Subcloud Evaporation section, we investigate the effect of subcloud evaporation on precipitation D-excess at this site.

When only the winter data were considered, the slope was closer to 8 (7.44; Table IV), consistent with the winter data plotting close to the GMWL. For the summer data on the other hand, slopes much less than 8 were seen. This indicates that the summer data have the larger influence on the annual LMWL. A slope lower than 8 was also obtained when the monthly precipitation weighted $\delta^{18}\text{O}$ and $\delta^2\text{H}$ values were calculated (Table IV).

Subcloud evaporation

The LMWL trends observed in the preceding sections suggest that subcloud evaporation is affecting the D-excess of the precipitation at this site. We investigate by how much using the model of Froehlich *et al.* (2008), which is fully documented by Kong *et al.* (2013). In the model, the evaporation of a raindrop as it falls below the cloud is estimated. Following this, the isotopic ratio modification in the falling raindrop is estimated using the relative humidity and the temperature of the atmosphere. In this application, we model equilibrium fractionation according to Horita and Wesolowski (1994). For this calculation, the cloud base is assumed at 1500 m above ground level (a.g.l.; this is a similar altitude to that used by Kong *et al.*, 2013). However, instead of using the temperature and humidity at ground level, a vertical temperature profile was used. We subdivide the altitude below the cloud in six vertical layers with boundaries at 200, 400, 600, 850, 1000, 1250 and 1500 m a.g.l. For the first 200 m a.g.l., the temperature and humidity obtained from the nearby BOM station were used (Coonamble airport; BOM station no. 051161), whereas for levels above this, the temperature and humidity were extracted from the GDAS files using HYSPLIT. The levels were chosen to correspond to the GDAS vertical resolution; however, HYSPLIT interpolates for the values at the selected points. An iterative procedure was then used where the fraction of raindrop remaining, after falling through each layer, was calculated working from the top layer down to the ground level (i.e. the new radius of the raindrop as it fell through a layer was recalculated from the fraction of raindrop remaining, and then the new radius together with the temperature and humidity of the next layer were used to determine the fraction of the raindrop remaining as it fell

through the next layer, etc. until it reached ground level). Following this, the isotopic exchange of the raindrop with the surrounding air was estimated where the temperature and relative humidity were a volume weighted average of the temperature and humidity in each level (where the volume was the volume of raindrop evaporated in each vertical layer).

Under the local conditions, the smallest raindrop that could be modelled with some precipitation still occurring at ground level was a raindrop of radius 1.0 mm. Marshall and Palmer (1948) reported raindrops between 0.5 and ~1.8 mm in radius. Thus, raindrops of radius 1.0 mm were selected to represent the smaller raindrops, and raindrops with radius of 1.5 mm were chosen to represent the larger raindrops.

For a raindrop with a radius of 1.0 mm, the smallest remaining fraction of the raindrop for all the samples was between 35.6 and 97.8%, with a mean of 81.6%. It was estimated that the measured D-excess at ground level was between 1.9 and 72.0‰ lower than what it was at cloud base (with a mean of 19.8‰, although there was one event with an increase of 104.6‰ – corresponding to an ^{18}O and ^2H -enriched summer sample). On the other hand, when using the surface-level temperature and humidity to estimate the D-excess increase at the base of the cloud, the range in the D-excess increase was 0.73 to 87.3‰, (excluding the previously identified ^{18}O and ^2H -enriched summer sample), indicating that overall, the subcloud evaporation was higher when the surface level conditions were used. However, when individual samples were considered, the estimated subcloud evaporation was higher when using the vertical levels in 100 out of the 282 cases, which could mostly be attributed to lower relative humidity at a number of levels above the surface. These results are consistent with previously reported values, e.g. we found a relationship of 1.2‰ decrease in D-excess per 1% evaporated fraction, which is similar to Salamalikis *et al.* (2016) and therein cited values from other studies.

Removing the samples for which the precipitation was less than 2 mm (i.e. samples that might have experienced some evaporation in the sampler) resulted in the same mean values for fraction of the remaining raindrop and change in D-excess, as when all the samples were used.

After correcting for subcloud evaporation, the OLSR-LMWL_{1500m} ($\delta^2\text{H}=6.1 \delta^{18}\text{O}+15.2$) still had a lower slope than the GMWL. This deviation from the GMWL suggests that at this site, aside from subcloud evaporation, other processes are forming the lower D-excess, e.g. a moisture source which has experienced some prior evaporation. To investigate this process, the isotopic difference of precipitation between moisture sourced over land and that sourced over the ocean was investigated (in the next section).

The change in D-excess, for all the samples, against the remaining fraction of the raindrop is presented in Figure 9, assuming the raindrops of radius 1.0 mm and 1.5 mm. The difference between the raindrops of different sizes is the fraction of evaporation; i.e. the larger the raindrops, the smaller the fraction of the raindrop evaporated and thus lower D-excess modification while the raindrops are falling below the cloud. For a raindrop with a radius of 1.5 mm, the remaining fraction of the raindrop for all the samples was between 64 and 99%, with a mean of 90%. The estimated range of the D-excess increase at the cloud level to that measured at the ground level was 1.17 to 36.0‰, with a mean of 11.2‰. After correcting for subcloud evaporation, the OLSR-LMWL_{1500m} ($\delta^2\text{H}=7.49 \delta^{18}\text{O}+18$) still had a lower slope than the GMWL.

Local and oceanic moisture sources

The isotopic composition of the source moisture can vary depending on the proportion of moisture sourced from the ocean surface and evapotranspiration from the land surface, e.g. transpiration returns moisture to the atmosphere with relatively little fractionation compared with the source water and therefore tends to be ^{18}O and ^2H -enriched relative to depleted vapour derived from the ocean (Zimmermann *et al.*, 1967; White and Gedzelman, 1984; Barnes and Allison, 1988; Wang and Yakir, 2000; Welp *et al.*, 2008; Jasechko *et al.*, 2013). While on longer timescales, transpiration can be considered a non-fractionating process, and more recently, a diurnal variation in the D-excess above plants has been observed (Welp *et al.*, 2012; Zhao *et al.*, 2014). Welp *et al.* (2012) reported that the peak-to-trough amplitude (in the diurnal

cycle) of the D-excess in the vapour varied between sites (e.g. 3.5‰ at Beijing and 7.7‰ at Luancheng).

Laboratory experiments for evaporation from soils have found that the isotopic composition of the water vapour is dependent on the time and depth of the soil evaporation front (Braud *et al.*, 2009a, b). Also, from studies in the Sahara desert, it is known that in arid regions, diffusive discharge of groundwater into the atmosphere from groundwater discharge points (e.g. springs) can occur (Araguás-Araguás and Froehlich, 1998; and references therein). In arid regions, the groundwater is often enriched in heavy isotopes relative to local meteoric waters (Araguás-Araguás and Froehlich, 1998); thus, any precipitation resulting from diffusive moisture would be more enriched with lower D-excess. In our study site, the average isotopic values of groundwater (measured in December 2007, February 2008, April 2008 and October 2008) were $\delta^{18}\text{O}$ of -3.41‰ and $\delta^2\text{H}$ of -22.7‰ , resulting in a D-excess of 4.58‰. However, we do not see that diffusive evaporation from the groundwater is likely, as the water table is deep ($\sim 10\text{ m}$) and the soils are predominantly clay. The $\delta^{18}\text{O}$ and $\delta^2\text{H}$ of the groundwater at this site were higher than reported for central Australia ($\delta^{18}\text{O}$ from -9.2 to -5.7‰ and $\delta^2\text{H}$ from -67 to -50‰ ; Harrington *et al.*, 2002), however, the precipitation weighted mean $\delta^{18}\text{O}$ and $\delta^2\text{H}$ of local precipitation at the Macquarie Marshes was -4.04 and -20.1‰ respectively, compared with the more depleted values of -6.3 and -33.8‰ respectively, at Alice Springs (Harrington *et al.*, 2002).

Local surface water, on the other hand, is much more enriched, with values that range from -2.0 and $+0.69\text{‰}$ and -15.6 to $+0.4\text{‰}$ for $\delta^{18}\text{O}$ and $\delta^2\text{H}$ respectively (giving a D-excess range of -5.12 to 0.4‰). Thus, the surface water could contribute to more enriched vapour with lower D-excess. Conversely, there is a small variation in the $\delta^{18}\text{O}$ of Australian marine surface waters ($\sim +0.1\text{‰}$ over the oceans to the east and west of the continent and $\sim -0.1\text{‰}$, in the Southern Ocean; Bigg and Rohling, 2000); thus, for moisture derived from the ocean, the $\delta^{18}\text{O}$ composition of the water vapour varies mainly with the sea surface temperature and relative humidity (Dansgaard, 1964; Majoube, 1971; Clark and Fritz, 1997; Uemura *et al.*, 2008; Lachniet, 2009).

To understand the source of moisture for this catchment, the percentage of moisture sourced over land (which can be from anywhere over the continent) was estimated for each sample, as described in the Back Trajectory and Trajectory Meteorological Data section. It was estimated that overall, 38% of the moisture was sourced over land (from the land surface, which is close to the estimated 40% of terrestrial precipitation originating from land evaporation; Van der Ent *et al.*, 2010). To investigate the effect of land sources *versus* oceanic sources of moisture, two groups of samples were

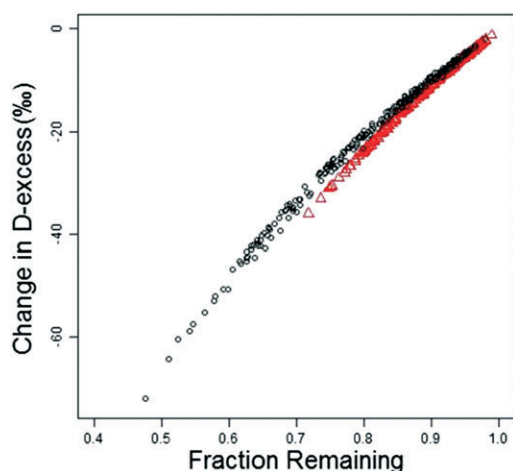


Figure 9. Reduction in D-excess (at ground level as a result of subcloud evaporation) against the remaining fraction of the raindrop for all the samples (with the one outlier removed; black circles: raindrop with a radius of 1.0 mm, red triangles: raindrop with a radius of 1.5 mm)

selected – those for which it was estimated that 75% or more of the moisture was sourced over the ocean, and the second where 75% or more of the moisture was sourced over land. The precipitation weighted averages of the selected variables within each group are presented in Table V. When the majority of moisture was sourced over land, (on average, at the moisture source) the temperature was higher (29 °C), and the relative humidity was lower (45%) than when moisture was sourced over the ocean (where the average temperature was 19 °C and the average humidity was 70%). The estimated relative humidity over the ocean is lower than that in the National Centre for Environmental Prediction reanalysis (Kalnay *et al.*, 1996; long-term mean of ~75 to ~80% off the east coast of Australia), which is most likely a result of the interpolation by HYSPLIT of the GDAS data files which are available on 1° × 1° resolution. If D-excess was affected by the conditions at the moisture source, this would imply that the D-excess would be lower when the majority of the moisture was sourced over the ocean. However, the D-excess was lower when the majority of moisture was sourced over land. This is most likely a result of this moisture being evaporated from surface water and overland transpiration. Decreasing D-excess in ground-level vapour has been observed, post-monsoon period, for a semi-arid site in India (Deshpande *et al.*, 2010), which they argued was a result of progressive enrichment of surface water and soil moisture. Subcloud evaporation would also contribute to overland moisture sources; however, this moisture would have a higher D-excess as moisture recycling increases the D-excess of the vapour (Froehlich *et al.*, 2008).

The samples for which more than 75% of the moisture was sourced over the ocean were ¹⁸O and ²H-depleted relative to those where 75% or more of the moisture was sourced over land. This further supports the possibility of vapour from previously evaporated surface water and transpiration contributing to precipitation when moisture was sourced over land. However, the air mass rainout occurring before the

Table V. Precipitation weighted average of selected variables for the two groups of samples – the first where 75% or more of the moisture was sourced over the ocean and the second where 75% or more of the moisture was sourced over land

	>75% ocean	>75% land
No. of samples	77	21
No. of samples winter	31	2
No. of samples summer	25	8
Temperature at moisture source (°C)	19	29
Relative humidity at moisture source (%)	70	45
Local surface relative humidity (%)	76	68
Average precipitation amount (mm)	11	11.6
Air mass prior cumulative rainfall (mm)	34.6	16
$\delta^{18}\text{O}$ (‰)	-5.2	-3.2
D-excess (‰)	12.5	12

Table VI. Precipitation weighted average values for samples immediately prior and after the higher rain events in 2010

	2009	2011
$\delta^{18}\text{O}$ (‰)	-4.37	-2.07
$\delta^2\text{H}$ (‰)	-22.0	-7.1
D-excess (‰)	12.9	9.5

precipitation at the site was higher when moisture was sourced over the ocean, thus further contributing to ¹⁸O and ²H-depleted precipitation signatures as a result of the rainout process (i.e. heavier isotopes raining out earlier).

Back trajectory analysis showed that the oceanic moisture was more likely to be sourced north-east of the site, and for those samples when the D-excess was below 0‰, the air masses were more likely to be arriving from the north-west quadrant (i.e. over the desert regions of Australia).

High precipitation occurred in the Macquarie Marshes in 2010 (a total of 1054 mm compared with 482 mm in 2009 and 487 mm in 2011), and subsequently, more surface water was available. The precipitation weighted isotopic values in precipitation for 2009 and then for 2011 are presented in Table VI. The difference in the means of the D-excess distributions before and after 2010 was significant at 95% confidence interval, indicating that evaporated surface water might have contributed to the precipitation for 2011.

CONCLUSIONS

Daily precipitation samples were collected (over a 7-year period; 2008–2014) at a semi-arid site located at the Macquarie Marshes, NSW (Australia). The samples were analysed for their isotopic (²H/¹H and ¹⁸O/¹⁶O) composition, and factors affecting the isotopic variability were investigated. The best correlation with $\delta^{18}\text{O}$ of precipitation was for local surface relative humidity, closely followed by the relative humidity at the moisture source, relative humidity in the air mass and cumulative rainout from the air mass prior to the site.

The precipitation weighted RMA local meteoric water line was calculated to be $\delta^2\text{H}=7.20 \delta^{18}\text{O}+9.1$ for the Macquarie Marshes. For comparison with the GMWL, the OLSR-derived LMWL was $\delta^2\text{H}=6.96 \delta^{18}\text{O}+6.4$. The lower slope and intercept are typical for warm dry sites, where subcloud evaporation of raindrops is experienced. This was further supported by the best correlation of the stable isotopes with local surface humidity, which would affect the partial evaporation of falling raindrops. When correcting for changes in isotopic composition as a result of subcloud evaporation, the modelled results for raindrops of 1.0 mm radius showed that on average, the measured D-excess was 19.8‰ lower than that at the base of the cloud,

and 18% of the moisture was evaporated before ground level. Once the correction was applied, a number of data points still plotted below the GMWL, indicating that some of the moisture was source from previously evaporated water, e.g. surface water, or transpiration.

Using back trajectory analysis, it was estimated that 38% of the moisture was sourced over land. The precipitation samples for which a larger proportion of the moisture was sourced over land were ^{18}O and ^2H -enriched with a lower D-excess in comparison to the samples for which the majority of the moisture was sourced over the ocean. These findings have implications for other inland semi-arid regions in the world.

ACKNOWLEDGEMENTS

We would like to thank Myra Tolhurst from Willie Retreat for the rainfall sample collection at the Macquarie Marshes. The authors would also like to thank various Australian Nuclear Science and Technology Organization personnel such as Barbora Gallagher and Scott Allchin for the $\delta^{18}\text{O}$ and $\delta^2\text{H}$ analysis. The NOAA Air Resources Laboratory made available the HYSPLIT transport and dispersion model and the relevant input files for generation of back trajectories.

REFERENCES

- Araguás-Araguás L, Froehlich K. 1998. Stable isotope composition of precipitation over southeast Asia. *Journal of Geophysical Research* **103** (D22): 28,721–28,742.
- Araguás-Araguás L, Froehlich K, Rozanski K. 2000. Deuterium and oxygen-18 isotope composition of precipitation and atmospheric moisture. *Hydrological Processes* **14**: 1341–1355.9.
- Awad MA. 1996. Application of stable isotopes (^{18}O , D) and geochemistry to study groundwater in Bahareya Oasis, Western Desert, Egypt. *Isotopes in Environmental and Health Studies* **32**: 87–95.
- Baldini LM, McDermott F, Baldini JUL, Fischer MJ, Mollhoff M. 2010. An investigation of the controls on Irish precipitation $\delta^{18}\text{O}$ values on monthly and event timescales. *Climate Dynamics* **35**: 977–993. DOI:10.1007/s00382-010-0774-6
- Bar-Matthews M, Ayalon A, Kaufman A. 1997. Late Quaternary paleoclimate in the Eastern Mediterranean region from stable isotope analysis of speleothems at Soreq Cave, Israel. *Quaternary Research* **47**: 155–168.
- Barnes CJ, Allison GB. 1988. Tracing of water movement in the unsaturated zone using stable isotopes of hydrogen and oxygen. *Journal of Hydrology* **100**: 143–176.
- Barras VJL, Simmonds I. 2008. Synoptic controls upon $\delta^{18}\text{O}$ in southern Tasmanian precipitation. *Geophysical Research Letters* **35**: L02707: DOI:10.1029/2007GL031835
- Barras V, Simmonds I. 2009. Observation and modelling of stable water isotopes as diagnostics of rainfall dynamics over southeastern Australia. *Journal of Geophysical Research* **114**: D23308: DOI:10.1029/2009JD012132
- Bigg GR, Rohling EJ. 2000. An oxygen isotope data set for marine waters. *Journal of Geophysical Research* **105**: 8527–8535.
- BOM 2012. MSLP maps sourced from the Australian Bureau of Meteorology at <http://www.bom.gov.au/australia/charts/archive/index.shtml>, (accessed in 2012).
- BOM 2015. Climate statistics of Australian locations — Quambone. http://www.bom.gov.au/climate/averages/tables/cw_051042.shtml (Accessed 29 Jul 2015)
- Braud P, Biron T, Bariac P, Richard P, Canale L, Gaudet JP, Vauclin M. 2009a. Isotopic composition of bare soil evaporated water vapour. Part I: RUBIC IV experimental set up and results. *Journal of Hydrology* **369**: 1–16.
- Braud T, Biron P, Vauclin M. 2009b. Isotopic composition of bare soil evaporated water vapour: part II: modeling of RUBIC IV experimental results. *Journal of Hydrology* **369**: 17–29.
- Burnett AW, Mullins HT, Patterson WP. 2004. Relationship between atmospheric circulation and winter precipitation $\delta^{18}\text{O}$ in central New York State. *Geophysical Research Letters* **31**: L22209: DOI:10.1029/2004GL021089
- Clark ID, Fritz P. 1997. *Environmental Isotopes in Hydrogeology*. CRC press: Boca Raton.
- Craig H. 1961. Isotopic variations in meteoric waters. *Science* **133**: 1702–1703.
- Crawford J, Hughes CE, Parkes SD. 2013. Is the isotopic composition of event based precipitation driven by moisture source or synoptic scale weather in the Sydney Basin, Australia? *Journal of Hydrology* **207**: 213–226.
- Crawford J, Hughes CE, Lykoudis S. 2014. Alternative least squares methods for determining the meteoric water line, demonstrated using GNIP data. *Journal of Hydrology* **519**: 2331–2340.
- Dansgaard W. 1964. Stable isotopes in precipitation. *Tellus* **16**: 436–468.
- Dansgaard W, Johnsen SJ, Clausen HB, Dahl-Jensen D, Gundestrup NS, Hammer CU, Hvidberg CS, Steffensen JP, Sveinbjornsdottir AE, Jouzel J, Bond G. 1993. Evidence for general instability of past climate from a 250-kyr ice-core record. *Nature* **364**: 218–220.
- Deshpande RD, Maurya AS, Kumar B, Sarkar A, Gupta K. 2010. Rain-vapor interaction and vapour identification using stable isotopes from semiarid western India. *Journal of Geophysical Research* **115**: D23311: DOI:10.1029/2009JD012799
- Draxler RR, Rolph GD. 2003. Hybrid Single-Particle Lagrangian Integrated Trajectory (HYSPLIT), model. <http://www.arl.noaa.gov/ready/hysplit4.html>.519, 2331–2340.
- Feng X, Faiia AM, Posmentier ES. 2009. Seasonality of isotopes in precipitation: a global perspective. *Journal of Geophysical Research* **114**: D08116: DOI:10.1029/2008JD011279
- Friedman I, Harris JM, Smith GI, Johnson CA. 2002. Stable isotope composition of waters in the Great Basin, United States 1. Air-mass trajectories. *Journal of Geophysical Research* **107**(D19): 4400: DOI:10.1029/2001JD000565
- Froehlich K, Kralik M, Papesch W, Pank D, Scheifinger H, Stichler W. 2008. Deuterium excess in precipitation of Alpine regions — moisture recycling. *Isotopes in Environmental and Health Studies* **44**: 1–10.
- Gat JP. 2000. Atmospheric water balance — the isotopic perspective. *Hydrological Processes* **14**: 1357–1369.
- Gat JR, Airey PL. 2006. Stable water isotopes in the atmosphere/biosphere/lithosphere interface: scaling from the local to continental scale, under humid and dry conditions. *Global and Planetary Change* **51**: 25–33.
- Gedzelman SD, Lawrence JR. 1990. The isotopic composition of precipitation from two extratropical cyclones. *Monthly Weather Review* **118**: 495–509.
- Gedzelman S, Lawrence J, Gamache J, Black M, Hindman E, Black R, Union J, Willoughby H, Zhang X. 2003. Probing hurricanes with stable isotopes of rain and water vapor. *Monthly Weather Review* **131**: 1112–1127.
- Guan H, Simmons CT, Love AJ. 2009. Orographic controls on rain water isotope distribution in the Mount Lofty Ranges of South Australia. *Journal of Hydrology* **374**: 255–264.
- Guan H, Zhang X, Skrzypek G, Sun Z, Xu X. 2013. Deuterium excess variations of rainfall events in a coastal area of South Australia and its relationship with synoptic weather systems and atmospheric moisture sources. *Journal of Geophysical Research, [Atmospheres]* **118**: 1–16. DOI:10.1002/jgrd.50137
- Harrington GA, Cook PG, Herczeg AL. 2002. Spatial and Temporal Variability of Ground Water Recharge in Central Australia: A Tracer Approach. *Ground Water* **40**: 518–528.
- Harvey FE, Welker JM. 2000. Stable isotopic composition of precipitation in the semi-arid north-central portion of the US Great Plains. *Journal of Hydrology* **238**: 90–109.
- Horita J, Wesolowski DJ. 1994. Liquid–vapour fractionation of oxygen and hydrogen isotopes of water from the freezing to the critical temperature. *Geochimica et Cosmochimica Acta* **58**: 3425–3437.
- Hughes CE, Crawford J. 2012. A new precipitation weighted method for determining the meteoric water line for hydrological applications demonstrated using Australian and global GNIP data. *Journal of Hydrology* **464**(465): 344–351.

- Hughes CE, Crawford J. 2013. Spatial and temporal variation in precipitation isotopes in the Sydney Basin, Australia. *Journal of Hydrology* **489**: 42–55.
- International Atomic Energy Agency. 1992. Statistical treatment of data on environmental isotopes in precipitation, Technical Reports Series No. 331. Vienna.
- International Atomic Energy Agency. 2005. Isotopic composition of precipitation in the Mediterranean Basin in relation to air circulation patterns and climate. IAEA-TECDOC-1453, IAEA, Vienna, ISBN 92-0-105305-1.
- Jacob H, Sonntag C. 1991. An 8-year record of the seasonal variation of 2H and 18O in atmospheric water vapour and precipitation at Heidelberg, Germany. *Tellus B* **43**: 291–300.
- Jasechko S, Sharp ZD, Gibson JJ, Birks SJ, Yi Y, Pawcett PJ. 2013. Terrestrial water fluxes dominated by transpiration. *Nature* **496**: 347–350. DOI:10.1038/nature11983
- Kalnay E, Kanamitsu M, Kistler R, Collins W, Deaven D, Gandin L, Iredell M, Saha S, White G, Woollen J, Chelliah M, Ebisuzaki W, Higgins W, Janowiak J, Mo KC, Ropelewski C, Wang J, Jenne R, Joseph D. 1996. The NCEP/NCAR 40-year reanalysis project. *Bulletin of the American Meteorological Society* **77**, 437–470. Data available at: <http://www.esrl.noaa.gov/psd/data/reanalysis/reanalysis.shtml>.
- Kong Y, Pang Z, Froehlich K. 2013. Quantifying recycled moisture fraction in precipitation of an arid region using deuterium excess. *Tellus B* **65**: 19251.
- Lachniet AS. 2009. Sea surface temperature control on the stable isotopic composition of rainfall in Panama. *Geophysical Research Letters* **36**: L03701; DOI:10.1029/2008GL036625
- Majoube M. 1971. Fractionnement en 18O et en deuterium entre l'eau et sa vapeur. *Journal of Chemical Physics* **10**: 1423–1428.
- Marshall JS, Palmer MK. 1948. The distribution of raindrops with size. *The Journal of Meteorology* **5**: 165–166.
- Matthews C, Geerts B. 1995. Characteristic thunderstorm distribution in the Sydney area. *Australian Meteorological Magazine* **44**: 127–138.
- Meredith KT, Hollins SE, Hughes CE, Cendon DI, Chisari R, Griffiths A, Crawford J. 2015. Understanding concentration and evaporation gradients created by episodic river recharge in a dry land aquifer using Cl , $\delta^{18}\text{O}$, $\delta^2\text{H}$, and ^3H . *Journal of Hydrology* **529**: 1070–1078.
- Merlivat L, Jouzel J. 1979. Global climatic interpretation of the deuterium-oxygen 18 relationship for precipitation. *Journal of Geophysical Research* **84**: 5029–5033.
- National Weather Services. 2015. http://www.cpc.ncep.noaa.gov/products/analysis_monitoring/ensostuff/ensoyears.shtml, accessed July 2015.
- Noone D, Simmonds I. 2002. Annual variations in moisture transport mechanisms and the abundance of $\delta^{18}\text{O}$ in Antarctic snow. *Journal of Geophysical Research* **107**: 4742; DOI:10.1029/2002JD002262
- Pang Z, Kong Y, Froehlich K, Huang T, Yuan L, Li Z, Wang F. 2011. Processes affecting isotopes in precipitation of an arid region. *Tellus B* **63**: 352–359.
- Peng H, Mayer B, Harris S, Krouse HR. 2007. The influence of below-cloud secondary effects on the stable isotope composition of hydrogen and oxygen in precipitation at Calgary, Alberta, Canada. *Tellus* **59**: 698–704.
- Peng TR, Wang CH, Huang CC, Fei LY, Chen CTA, Hwong JL. 2010. Stable isotopic characteristic of Taiwan's precipitation: a case study of western Pacific monsoon region. *Earth and Planetary Science Letters* **289**: 357–366. DOI:10.1016/j.epsl.2009.11.024
- Salamalikis V, Argiriou AA, Dotsika E. 2016. Isotopic modelling of the sub-cloud evaporation effect in precipitation. *Science of the Total Environment* **544**: 1059–1072.
- Samuels-Crow KE, Galewsky J, Hardy DR, Sharp ZD, Worden J, Braun C. 2014. Upwind convective influences on the isotopic composition of atmospheric water vapor over the tropical Andes. *Journal of Geophysical Research, [Atmospheres]* **119**: 7051–7063. DOI:10.1002/2014JD021487
- Scholl MA, Shanley JB, Zegarra JP, Coplen TB. 2009. The stable isotope amount effect: new insights from NEXRAD echo tops, Luquillo Mountains, Puerto Rico. *Water Resources Research* **45**: W12407; DOI:10.1029/2008WR007515
- Sinclair KE, Bertler NAN, Trompette WJ, Baisden WT. 2013. Seasonality of air mass pathways to Coastal Antarctica: ramifications for interpreting high-resolution ice core records. *Journal of Climate* **26**: 2065–2076.
- Sjostrom DJ, Welker JM. 2009. The influence of air mass source on the seasonal isotopic composition of precipitation, eastern USA. *Journal of Geochemical Exploration* **102**: 103–112.
- Sodemann H, Schwierz C, Wernli H. 2008. Interannual variability of Greenland winter precipitation sources: Lagrangian moisture diagnostic and North Atlantic Oscillation influence. *Journal of Geophysical Research* **113**: D03107; DOI:10.1029/2007JD008503
- Speer MS, Wiles P, Pepler A. 2009. Low pressure systems off the New South Wales coast and associated hazardous weather: establishment of a database. *Australian Meteorological and Oceanographic Journal* **58**: 29–39.
- Stewart MK. 1975. Stable isotope fractionation due to evaporation and isotopic exchange of falling water drops: applications to atmospheric processes and evaporation of lakes. *Journal of Geophysical Research* **80**: 1133–1146.
- Tan M. 2014. Circulation effect: response of precipitation $\delta^{18}\text{O}$ to the ENSO cycle in monsoon regions of China. *Climate Dynamics* **42**: 1067–1077.
- Treble PC, Budd WF, Hope PK, Rustonji PK. 2005. Synoptic-scale climate patterns associated with rainfall $\delta^{18}\text{O}$ in southern Australia. *Journal of Hydrology* **302**: 270–282.
- Trenberth KE. 1998. Atmospheric moisture residence times and cycling: implications for rainfall rates and climate change. *Climatic Change* **39**: 667–694.
- Uemura R, Matsui Y, Yoshimura K, Motoyana H, Yoshida N. 2008. Evidence of deuterium excess in water vapour as an indicator of ocean surface conditions. *Journal of Geophysical Research, [Atmospheres]* **113**: D19114; DOI:10.1029/2008JD010209
- Vachon RW, Welker JM, White WC, Vaughn BH. 2010. Moisture source temperatures and precipitation $\delta^{18}\text{O}$ -temperature relationships across the United States. *Water Resources Research* **46**: W07523; DOI:10.1029/2009WR008558
- Van der Ent RJ, Savenije HHG, Schaeffli B, Steele-dunne SC. 2010. Origin and fate of atmospheric moisture over continents. *Water Resources Research* **46**: W09525; DOI:10.1029/2009WR008558
- Vimeux F, Masson V, Jouzel J, Petit JR, Steig EJ, Stievenard M, Vaikmae R, White JWC. 2001. Holocene hydrological cycle changes in the Southern Hemisphere documented in East Antarctic deuterium excess records. *Climate Dynamics* **17**: 503–513.
- Wang XF, Yakir D. 2000. Using stable isotopes of water in evapotranspiration studies. *Hydrological Processes* **14**: 1407–1421.
- Welp LR, Lee X, Kim K, Griffis TJ, Billmark KA, Baker JM. 2008. $\delta^{18}\text{O}$ of water vapour, evapotranspiration and the sites of leaf water evaporation in a soybean canopy. *Plant, Cell and Environment* **31**: 1214–1228. DOI:10.1111/j.1365-3040.2008.01826.x
- Welp LR, Lee X, Griffis TJ, Wen X-F, Xiao W, Li S, Sun X, Hu Z, Martin MV, Huang J. 2012. A meta-analysis of water deuterium-excess in the midlatitude atmospheric surface layer. *Global Biogeochemical Cycles* **26**: GB3021; DOI:10.1029/2011GB004201
- Wen L, Macdonald R, Morrison T, Hameed T, Saintilan N, Ling J. 2013. From hydrodynamic to hydrological modelling: investigating long-term hydrological regimes of key wetlands in the Macquarie Marshes, a semi-arid lowland floodplain in Australia. *Journal of Hydrology* **500**: 45–61.
- White JWC, Gedzelman D. 1984. The isotopic composition of atmospheric water vapour and the concurrent meteorological conditions. *Journal of Geophysical Research* **89**: 4937–4939.
- Windhorst D, Waltz T, Frede H-G, Breuer L. 2012. Impact of elevation and weather patterns on the isotopic composition of precipitation in a tropical montane rainforest. *Hydrological and Earth System Sciences Discussions* **9**: 8425–8453. DOI:10.5194/hessd-9-8425-2012
- Yoshimura K, Kanamitsu M, Dettlinger M. 2010. Regional downscaling for stable water isotopes: a case study of an atmospheric river event. *Journal of Geophysical Research* **115**: D18114; DOI:10.1029/2010JD014032
- Zhao L, Wang L, Liu X, Xiao H, Ruan Y, Zhou M. 2014. The patterns and implications of diurnal variations in the d-excess of plant water, shallow soil water and soil moisture. *Hydrological and Earth System Sciences* **18**: 4129–4151.
- Zimmermann U, Ehhalt D, Munnich K. 1967. Soil water movement and evapotranspiration change in the isotopic composition of water. In *Isotopes in Hydrology*. International Atomic Energy Agency: Vienna, Austria; 567–585.

SUPPORTING INFORMATION

Additional supporting information may be found in the online version of this article at the publisher's web-site.